Proc. Indian Acad. Sci. (Math. Sci.) Vol. 116, No. 3, August 2006, pp. 361–371.

The embedding method for linear partial differential equations in unbounded and multiply connected domains

P N SHANKAR

National Aerospace Laboratories, Bangalore 560 017, India
E-mail: pn_shankar55@rediffmail.com

MS received 20 January 2006

Abstract. The recently suggested embedding method to solve linear boundary value problems is here extended to cover situations where the domain of interest is unbounded or multiply connected. The extensions involve the use of complete sets of exterior and interior eigenfunctions on canonical domains. Applications to typical boundary value problems for Laplace's equation, the Oseen equations and the biharmonic equation are given as examples.

Keywords. Partial differential equations; boundary value problems; the embedding method; unbounded and multiply connected domains.

1. Introduction

A way to extend the method of eigenfunction expansions to handle boundary value problems for linear operators in essentially arbitrary domains was recently suggested in [4]. The basic idea is to embed the given bounded domain $\mathcal{D}$ of complex shape in a canonical domain $\hat{\mathcal{D}}$ which has a complete set of eigenfunctions of the operator $\mathcal{L}$. These eigenfunctions can then be superposed to solve boundary value problems for $\mathcal{L}$ in the given domain $\mathcal{D}$. The expansion coefficients can be obtained by a least-squares procedure which minimizes the errors in the data on the boundary $\mathcal{B}$ of $\mathcal{D}$.

Restrictions in the above work were that the given domain $\mathcal{D}$ had to be bounded and simply connected. We wish to remove these restrictions in this brief communication. The resulting extensions of the method will considerably increase the scope of the technique. For example, conduction problems involving unbounded domains and external fluid flows past bodies now come within its scope, as do transport processes involving cut-outs and bounded flows past obstructions. The extensions are given in §2 and these are illustrated by examples in §3.

2. The extension to unbounded and multiply connected domains

Let $\hat{\mathcal{B}}$ be the boundary of a bounded, simply connected domain $\hat{\mathcal{D}}$ in R^2 or R^3. It will be useful to define the interior and exterior eigenfunctions of an operator $\mathcal{L}$ with respect to the boundary $\hat{\mathcal{B}}$ in some coordinate system. Let the set $\hat{\Phi}^i(\hat{\mathcal{B}}) = \{\hat{\phi}^i_n(\mathbf{x}),\ n = 1, 2, \dots\}$ of eigenfunctions of $\mathcal{L}$ be defined and bounded in the interior of $\hat{\mathcal{D}}$ and be complete in the sense of [4]. The set $\hat{\Phi}^i(\hat{\mathcal{B}})$ will be called the set of interior eigenfunctions of $\mathcal{L}$ with respect to $\hat{\mathcal{B}}$. Thus, if $\hat{\mathcal{B}}$ is a circle in the plane and $\mathcal{L}$ is the Laplacian, $r^n \exp in\theta$ is an

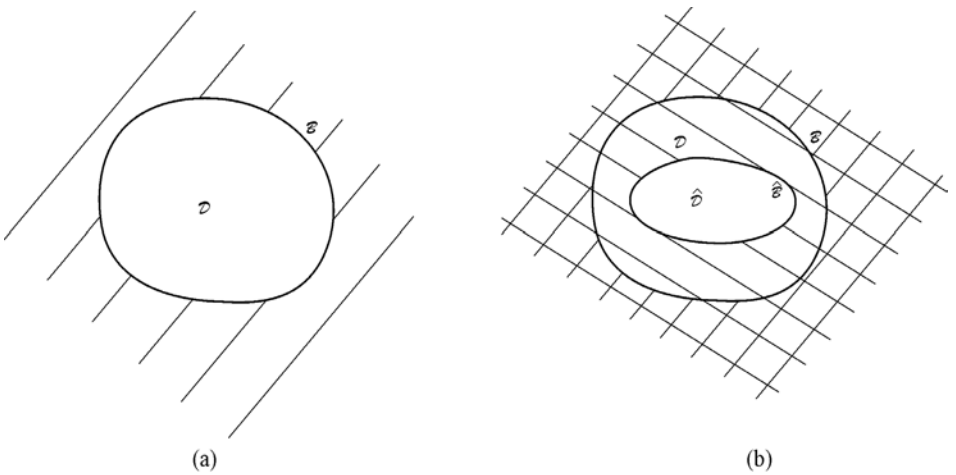

Figure 1. The embedding method for exterior, unbounded domains. **(a)** The domain of interest is exterior to the bounded domain $\mathcal{D}$ with boundary $\mathcal{B}$. **(b)** The exterior of the nice domain $\hat{\mathcal{D}}$ with boundary $\hat{\mathcal{B}}$, contains the exterior of $\mathcal{D}$.

interior eigenfunction for integer n. Similarly, let the set $\hat{\Phi}^e(\hat{\mathcal{B}}) = \{\hat{\phi}_n^e(\mathbf{x}),\ n = 1, 2, \dots\}$ of eigenfunctions of $\mathcal{L}$ be defined and bounded[1] in the exterior of $\hat{\mathcal{D}}$ and be complete in the sense above. This set will be called the set of exterior eigenfunctions with respect to $\hat{\mathcal{B}}$. For the Laplacian exterior to a disc, $r^{-n} \exp in\theta$ is an exterior eigenfunction for integer n. We will usually not indicate the dependence on $\hat{\mathcal{B}}$ as this will be clear from the context.

Suppose we wish to solve the linear equation

$$\mathcal{L}\psi(\mathbf{x}) = 0 \tag{2.1}$$

exterior to the bounded, simply connected domain $\mathcal{D}$ shown in figure 1a with suitable boundary conditions on $\mathcal{B}$[2]. We assume that the problem posed has a unique solution; moreover, the boundary $\mathcal{B}$ of the body is a simple curve or surface. Let us suppose that $\mathcal{D}$ is such that it does not possess, or appears not to possess, a complete set of exterior eigenfunctions $\{\phi_n^e(\mathbf{x}),\ n = 1, 2, \dots\}$. Let us further suppose that there is a domain $\hat{\mathcal{D}}$ with boundary $\hat{\mathcal{B}}$ for which a complete set of exterior eigenfunctions $\{\hat{\phi}_n^e(\mathbf{x}),\ n = 1, 2, \dots\}$ exists in some suitable coordinate system. Then the embedding method for exterior domains consists in embedding the domain $\hat{\mathcal{D}}$ with boundary $\hat{\mathcal{B}}$ *inside* the given body with boundary $\mathcal{B}$. This can always be done by scaling and translation. The situation will then be as shown in figure 1b. Now note that the exterior of $\hat{\mathcal{B}}$ now embeds or contains the exterior of $\mathcal{B}$. This suggests that we can use the eigenfunctions of the embedded domain with boundary $\hat{\mathcal{B}}$ to solve the problem exterior to the given domain $\mathcal{D}$. Consequently, to solve (2.1) in $\mathcal{D}^c$ subject to suitable boundary conditions on $\mathcal{B}$, we write

$$\psi(\mathbf{x}) = \Re \sum_{n=1}^{\infty} a_n \hat{\phi}_n^e(\mathbf{x}), \tag{2.2}$$

[1]There are exceptional cases where a mild growth of the functions is permitted. Examples are given in §3.

[2]Here $\psi(\mathbf{x})$ has been assumed to be a scalar field. But exactly the same arguments go through if it is a vector field.

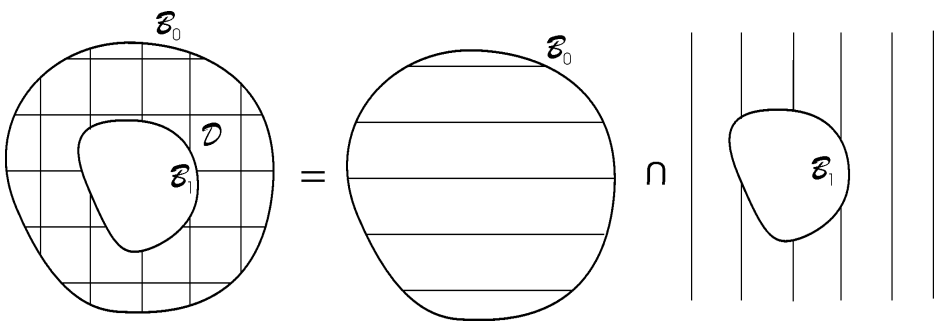

Figure 2. The embedding method for multiply connected domains. The given domain $\mathcal{D}$ has boundaries $\mathcal{B}_0$ and $\mathcal{B}_1$ and is the intersection of the domain interior to $\mathcal{B}_0$ and the domain exterior to $\mathcal{B}_1$.

where a_n, $n = 1, 2, \ldots$, are in general complex scalars that have to be determined so that the boundary conditions on $\mathcal{B}$ are satisfied. This can always be done by the least-squares procedure [4]. This generalizes the embedding method to exterior domains.

Consider the multiply connected domain $\mathcal{D}$ in R^2 shown in figure 2 with interior boundary $\mathcal{B}_1$ and outer boundary $\mathcal{B}_0$. We wish to solve (2.1) in this domain subject to suitable boundary conditions on $\mathcal{B}_1$ and $\mathcal{B}_0$. We note from the right-hand side of figure 2 that the given domain is just the intersection of the interior of $\mathcal{B}_0$ and the exterior of $\mathcal{B}_1$. This immediately suggests that we need to use a set of interior eigenfunctions whose domain includes the interior of $\mathcal{B}_0$ together with a set of exterior eigenfunctions whose domain includes the exterior of $\mathcal{B}_1$. Let $\Phi^i(\mathcal{B}_0^*)$ and $\Phi^e(\mathcal{B}_1^*)$ be sets of interior and exterior eigenfunctions of $\mathcal{L}$; the stars indicate that in general the eigenfunctions derive from boundaries other than the given ones. Then we claim that the Φ given by

$$\Phi = \Phi^i(\mathcal{B}_0^*) \bigcup \Phi^e(\mathcal{B}_1^*) \tag{2.3}$$

will be a complete set of eigenfunctions capable of solving (2.1) in $\mathcal{D}$ subject to the given data on $\mathcal{B}_0$ and $\mathcal{B}_1$[3].

A check on the consistency of the above procedure can be made by considering the limiting cases. If $\mathcal{B}_0$ is gradually moved to infinity, we will just have the exterior problem for $\mathcal{B}_1$. The contributions from $\Phi^i(\mathcal{B}_0^*)$ will vanish but $\Phi^e(\mathcal{B}_1^*)$ will remain to handle the exterior problem. On the other hand, if the inner boundary vanishes $\Phi^i(\mathcal{B}_0^*)$ will handle the interior problem for $\mathcal{B}_0$.

That both sets are necessary can be seen from another argument. With given boundary conditions on $\mathcal{B}_0$, the set $\Phi^i(\mathcal{B}_0^*)$ will uniquely determine data on the inner boundary $\mathcal{B}_1$ which will in general not match the data given on it. Hence the need for the set $\Phi^e(\mathcal{B}_1^*)$.

In summary the expansion

$$\psi(\mathbf{x}) = \Re \sum_{n=1}^{\infty} a_n \phi_n(\mathbf{x}), \tag{2.4}$$

[3]There is, however, a small but important caveat. If part of the embedding boundary $\mathcal{B}_0^*$ is not smooth, it may be necessary to include in (2.3) general solutions of (2.1) Φ^g, in order to cancel out inhomogeneous data at these corners (see [3]). Examples of such cases are given in §3.

where $\phi_n(\mathbf{x})$ are the elements of Φ defined by (2.3), is expected to solve the boundary value problem in the multiply connected domain $\mathcal{D}$. As before, the coefficients a_n can be determined by the least-squares procedure.

A similar argument shows that if the domain $\mathcal{D}$ is k-ply connected, rather than doubly connected, we will need k sets of exterior eigenfunctions and (2.3) would have to be replaced by

$$\Phi = \Phi^i(\mathcal{B}_0^*) \bigcup \Phi^e(\mathcal{B}_1^*) \bigcup \cdots \bigcup \Phi^e(\mathcal{B}_k^*). \tag{2.5}$$

It also follows that if there is no exterior boundary, i.e. if $\mathcal{B}_0$ moves to infinity, only the first term $\Phi^i(\mathcal{B}_0^*)$ in the above union needs to be dropped. This result also holds in R^3.

In the next section we will consider a number of examples which will make these extensions very clear.

3. Examples of fields in unbounded and multiply connected domains

In the examples that follow no attempt has been made to optimize the calculations or to get very high accuracy. The particular choices of complex domain shapes have been dictated primarily by convenience: often, the most tedious part of a calculation is the specification of the complex geometry.

3.1 *Laplace's equation exterior to a truncated sphere: Steady, three-dimensional heat conduction*

Consider the three-dimensional temperature field $\psi(r, \theta, \phi)$ exterior to a truncated sphere as shown in figure 3. In the figure, the polar axis is vertically upwards with the surface of the body being spherical, of unit radius, for $\theta > \alpha$; for $\theta \leq \alpha$ the surface is flat with the radius being given by $r = r_B(\theta) = \cos\alpha / \cos\theta$. Exterior to the body the field satisfies Laplace's equation

$$\nabla^2 \psi(r, \theta, \phi) = 0. \tag{3.1}$$

If the far-field is at zero temperature, we require $\psi(r, \theta, \phi) \to 0$ as $r \to \infty$, while on the body it will have to take on the given temperature distribution. It is sufficient to consider surface temperature distributions, $\psi_B(\theta, \phi)$, of the form

$$\psi_B(\theta, \phi) = f(\theta) \cos m\phi, \tag{3.2}$$

where m is the azimuthal mode number and $f(\theta)$ is arbitrary.

For this body geometry, it is natural in the embedding method to embed in the given body a smaller sphere and use the exterior eigenfunctions of the sphere. We can then immediately write down an eigenfunction expansion to solve (3.1) subject to the given boundary conditions:

$$\psi(r, \theta, \phi) = \cos m\phi \sum_{n=m}^{\infty} a_n r^{-n-1} P_n^m(\cos\theta), \tag{3.3}$$

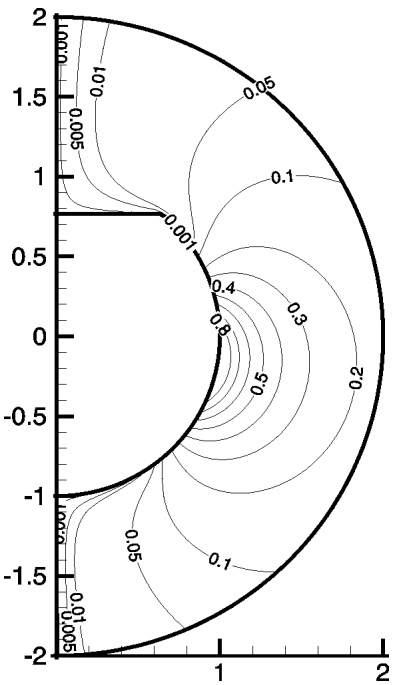

Figure 3. Heat conduction exterior to a truncated sphere. The isotherms in the plane $\phi = 0$ when $m = 1$. $\alpha = 40^\circ$, $\theta_0 = 50^\circ$ and $\theta_1 = 150^\circ$.

where $P_n^m(\cos\theta)$ is the associated Legendre function of degree n, order m and argument $\cos\theta$. On the boundary of the section given by $r = r_B(\theta)$, the condition (3.2) requires

$$\sum_{n=m}^{\infty} a_n r_B^{-n-1}(\theta) P_n^m(\cos\theta) = f(\theta), \quad 0 \le \theta \le \pi. \tag{3.4}$$

The real scalars a_n can be determined to any required accuracy by a least-squares procedure that minimizes the error in satisfying (3.4) over the whole boundary [4]. The sum is truncated to N terms and the minimization is carried out over $M > N$ points on the boundary.

For the example considered in figure 3, m was 1 and the surface temperature distribution was given by

$$f(\theta) = \begin{cases} 0, & 0 \le \theta < \theta_0,\ \theta_1 < \theta \le \pi \\ \frac{1}{2}\left[1 + \cos\left\{\frac{\pi}{\theta_1 - \theta_0}(2\theta - (\theta_1 + \theta_0))\right\}\right], & \theta_0 \le \theta \le \theta_1 \end{cases}. \tag{3.5}$$

For the case shown, 50 terms in the sum were used with 100 minimization points. The maximum error on the boundary was about 0.22×10^{-2} while the errors were at least an order of magnitude smaller at most other points. The maximum errors occur not at the sharp edge on the boundary but where the given temperature distribution suffers a certain loss of smoothness, i.e. near $\theta = \theta_0$ and $\theta = \theta_1$.

3.2 *The planar Oseen equations: Slow viscous flow past a bluff body*

We next consider, as another example of an exterior field, planar low Reynolds number flow past a bluff body as modelled by the Oseen equations. Although the spatial dimension is lower, this is a more complicated example since the equation is of a higher order and the relevant eigenfunctions are less well-known.

Consider steady, slow, planar, viscous flow past a cylindrical, bluff body with boundary $\mathcal{B}$. The uniform fluid velocity at infinity is U and the body has a length scale L associated with it. Assume that all quantities are non-dimensionalized by these scales and define the Reynolds number $\mathrm{Re} = \rho UL/\mu$. A stream function $\psi(x, y)$ exists, from which the velocity components are given by $u_x = \psi_{,y}$ and $u_y = -\psi_{,x}$. The momentum equations can then be written for each component as

$$\mathrm{Re}\,\psi_{,yx} = -p_{,x} + \nabla^2\psi_{,y} \tag{3.6a}$$

$$-\mathrm{Re}\,\psi_{,xx} = -p_{,y} - \nabla^2\psi_{,x} \tag{3.6b}$$

which on elimination of the pressure yield a single scalar equation

$$\mathcal{L}_1\mathcal{L}_2\psi(x, y) = \nabla^2\left(\nabla^2 - \mathrm{Re}\frac{\partial}{\partial x}\right)\psi(x, y) = 0 \tag{3.7}$$

for the stream function.

The boundary conditions to be imposed on the field are the no-slip and no-penetration conditions on the body boundary $\mathcal{B}$ and recovery to uniform flow in the far-field:

$$\psi_{,y}(\text{on } \mathcal{B}) = \psi_{,x}(\text{on } \mathcal{B}) = 0, \tag{3.8a}$$

$$\psi_{,y}(r \to \infty) = 1, \quad \psi_{,x}(r \to \infty) = 0. \tag{3.8b}$$

For the embedding method, we will use the circle as a suitable embedded boundary because the circular cylinder has a convenient, complete set of exterior eigenfunctions. Filon [1], in another context, derived a general far-field expansion for the Oseen equations. In our notation this expansion takes the form

$$\psi(r, \theta) = \psi_1(r, \theta) + \psi_2(r, \theta), \tag{3.9}$$

where

$$\psi_1(r, \theta) = r\sin\theta - b_0\theta + c_0\ln r + \sum_{n=1}\left(\frac{r^*}{r}\right)^n\{a_n\sin n\theta + c_n\cos n\theta\}, \tag{3.10a}$$

$$\begin{aligned}\psi_2(r, \theta) = b_0\Bigg[\beta r\int_0^\theta\{K_1(\beta r) + K_0(\beta r)\cos\chi\}\mathrm{e}^{\beta r\cos\chi}\,\mathrm{d}\chi\Bigg] \\ + d_0\mathrm{e}^{\beta r\cos\theta}K_0(\beta r) \\ + \sum_{n=1}\Bigg[\mathrm{e}^{\beta r\cos\theta}\frac{K_n(\beta r)}{K_n(\beta r^*)}\{b_n\sin n\theta + d_n\cos n\theta\}\Bigg],\end{aligned} \tag{3.10b}$$

where the real scalars b_0, c_0, d_0 and a_n, b_n, c_n and d_n, $n = 1, 2, \ldots$ have yet to be determined. $K_n(\beta r)$ is the modified Bessel function of order n and argument βr which

vanishes at infinity; $\beta = \mathrm{Re}/2$ and r^* is a scale that can be set to 1. Note that ψ_1 and ψ_2 are the solutions to $\mathcal{L}_1\psi(x, y) = 0$ and $\mathcal{L}_2\psi(x, y) = 0$ respectively in (3.7). The velocity components are given by

$$\begin{aligned} u_r(r,\theta) = \cos\theta &+ b_0\left[\beta\{K_1(\beta r) + K_0(\beta r)\cos\theta\}\mathrm{e}^{\beta r\cos\theta} - \frac{1}{r}\right] \\ &- d_0\beta\mathrm{e}^{\beta r\cos\theta}K_0(\beta r)\sin\theta \\ &+ \sum_{n=1}\left[\frac{n}{r}\left(\frac{r^*}{r}\right)^n\{a_n\cos n\theta - c_n\sin n\theta\}\right. \\ &+ \mathrm{e}^{\beta r\cos\theta}\frac{K_n(\beta r)}{K_n(\beta r^*)}\left\{b_n\left(\frac{n\cos n\theta}{r} - \beta\sin\theta\sin n\theta\right)\right. \\ &\left.\left. -d_n\left(\frac{n\sin n\theta}{r} + \beta\sin\theta\cos n\theta\right)\right\}\right], \end{aligned} \tag{3.11a}$$

$$\begin{aligned} u_\theta(r,\theta) = -\sin\theta &- b_0\{\beta K_0(\beta r)\sin\theta\mathrm{e}^{\beta r\cos\theta}\} \\ &- \frac{c_0}{r} + d_0\beta\mathrm{e}^{\beta r\cos\theta}\{K_1(\beta r) - K_0(\beta r)\cos\theta\} \\ &- \sum_{n=1}\left[-\frac{n}{r}\left(\frac{r^*}{r}\right)^n\{a_n\sin n\theta + c_n\cos n\theta\}\right. \\ &\left. +\mathrm{e}^{\beta r\cos\theta}\frac{\beta\cos\theta K_n(\beta r) + K_n'(\beta r)}{K_n(\beta r^*)}\{b_n\sin n\theta + d_n\cos n\theta\}\right]. \end{aligned} \tag{3.11b}$$

The method then consists of assuming the expansions (3.10) to hold for the exterior of $\mathcal{B}$. The conditions at infinity are already satisfied. One then only has to satisfy the no-slip conditions (3.8a) on the body. This is done by a least-squares approach as before. The sums in (3.10) are truncated to N terms and the $4N + 3$ coefficients are determined such that the errors in the boundary conditions are minimized at $M > 4N + 3$ points on $\mathcal{B}$. It is expected that as $N, M \to \infty$ the solution will tend to be independent of N and M and converge to the exact solution.

The method was first tested for the circular cylinder itself; the results were found to be in excellent agreement over a range of Re with those of Miyagi [2], who had used a surface singularity, integral equation method. Subsequently, the method was applied to a body section, shaped like a space re-entry capsule, shown in figure 4 to obtain the streamline patterns that are displayed in the figure. At zero angle of attack, when the body shape is symmetric about the x-axis with the apex lying on it, the body shape is given by the general parametric representation

$$x = p_0\cos\tau, \quad y = q_0\sin\tau + q_1\sin 2\tau \quad 0 \le \tau < 2\pi. \tag{3.12}$$

For the particular case shown, $p_0 = q_0 = 0.5, q_1 = -0.2$, while the Reynolds number $\mathrm{Re} = 0.5$ and the angle of attack $\alpha = 30^\circ$. The flow appears to be fully attached. The lift and drag coefficients, based on $\rho U^2 L/2$, are approximately -0.458 and 18.82 respectively. Using $N = 50$ and $M = 300$ the maximum errors on the boundary were approximately

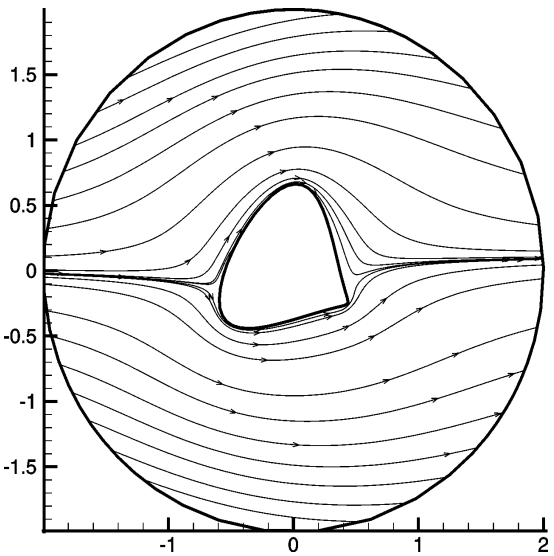

Figure 4. Slow viscous flow past a body according to the Oseen equations. The body shape is given by (3.12) with $p_0 = q_0 = 0.5$ and $q_1 = -0.2$. The Reynolds number and angle of attack are Re $= 0.5$ and $\alpha = 30^\circ$.

0.55×10^{-2} and 0.89×10^{-2}; naturally these were in the neighbourhood of the trailing edge. And, as usual, the errors over most other points were an order of magnitude smaller.

3.3 *Laplace's equation in a multiply-connected domain: Planar heat conduction*

Figure 5a shows a multiply connected domain in the plane. The outer boundary is the same as the one considered in figure 2 of [4]: three sides of a rectangle together with a semi-circle BCD of unit radius. Inside, is a circular cut-out of radius r_1 centred at (x_c, y_c) with respect to the origin at O at the lower left corner. We wish to determine the temperature distribution $\psi(x, y)$ in the section given data on the inner and outer boundaries.

The field satisfies Laplace's equation (3.1) in the multiply connected domain. According to the discussion in §2 the eigenfunction expansion will consist of a set of interior eigenfunctions of the type considered in §3(a) of [4] together with an exterior set for the cut-out. Here we embed the domain in the rectangle AFGO shown in figure 5a. Thus we are led to the representation

$$\psi(x, y) = \psi^i(x, y) + \psi^e(r', \theta') + \psi^g(x, y), \tag{3.13}$$

where

$$\psi^i(x, y) = \sum_{n=1}^{N_1} [\sin \lambda_n x \{a_n e^{-\lambda_n (2-y)} + b_n e^{-\lambda_n y}\} + \sin \mu_n y \{c_n e^{-\mu_n (h_1 - x)} + d_n e^{-\mu_n x}\}], \tag{3.14a}$$

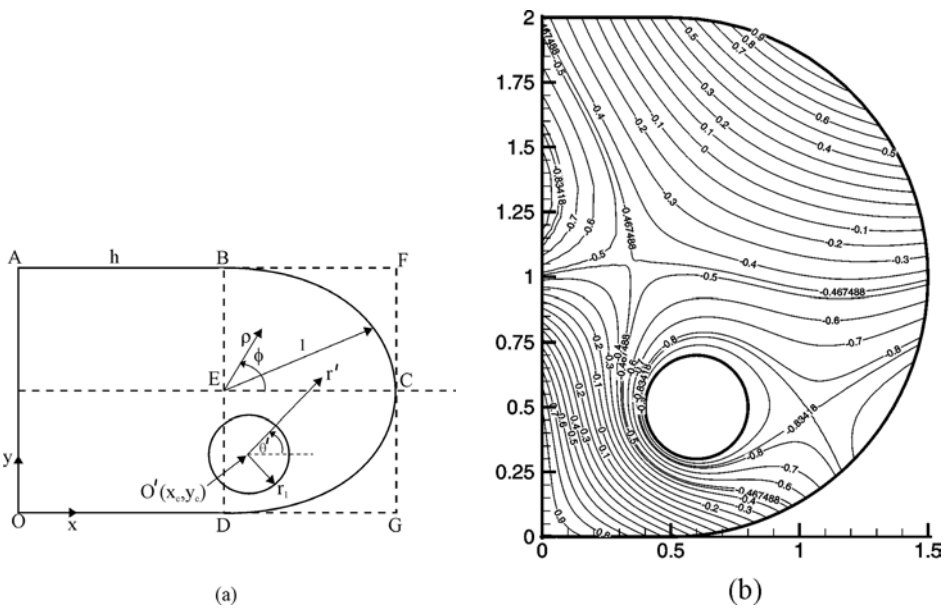

Figure 5. Heat conduction in a multiply connected domain. **(a)** A schematic and **(b)** isotherms. The temperature on the outer boundary is given by $g_o(\phi) = \cos 2(\phi - \phi_0)$ while on the circular inner boundary $g_i(\theta') = -1$. $h = 0.5$, $r_1 = 0.2$, $x_c = 0.6$, $y_c = 0.5$, $\phi_0 = 45 \approx 58.31^\circ$.

$$\psi^e(r', \theta') = e_0 + f_0 \ln r' + \sum_{n=1}^{N_2} \left(\frac{r'}{r_1}\right)^{-n} \{e_n \cos n\theta' + f_n \sin n\theta'\}, \quad (3.14b)$$

$$\psi^g(x, y) = a_0 x + b_0 y. \quad (3.14c)$$

In the above $h_1 = h + 1$, $\lambda_n = n\pi/h_1$, $\mu_n = n\pi/2$ where $n = 1, 2, \ldots$.

It should be noted that (i) the two terms in (3.14c), general solutions of the field equations, are necessary to cancel inhomogeneous data at the corners A and O [3], (ii) the first two terms in (3.14b) show that this is one of the exceptional cases where even a small growth at infinity is tolerated in the external eigenfunctions and (iii) the number of terms in the sums in (3.14a) and (3.14b) need not be equal. Now if $g_o(\phi)$ and $g_i(\theta')$ are the given data on the outer and inner boundaries, the $4N_1 + 2N_2 + 4$ unknowns can be determined by minimizing the errors at M points on the complete boundary. Figure 5b shows the isotherms for a particular set of parameters. In this case $N_1 = N_2 = N = 20$ and M was 160; the maximum error was approximately 0.58×10^{-4}.

3.4 *Planar Stokes flow in a multiply connected domain*

Consider steady planar Stokes flow in a rectangular container with a stirrer of circular section that can rotate. A sketch of the configuration is shown in figure 6a. The viscous liquid that fills the container is kept in motion both by the movement of the lid with speed $u_0(x)$, symmetric about $x = 1/2$, and the rotation of the stirrer with angular velocity ω_0. The container is of unit width and depth h while the radius of the stirrer is r_0. As in §3.2,

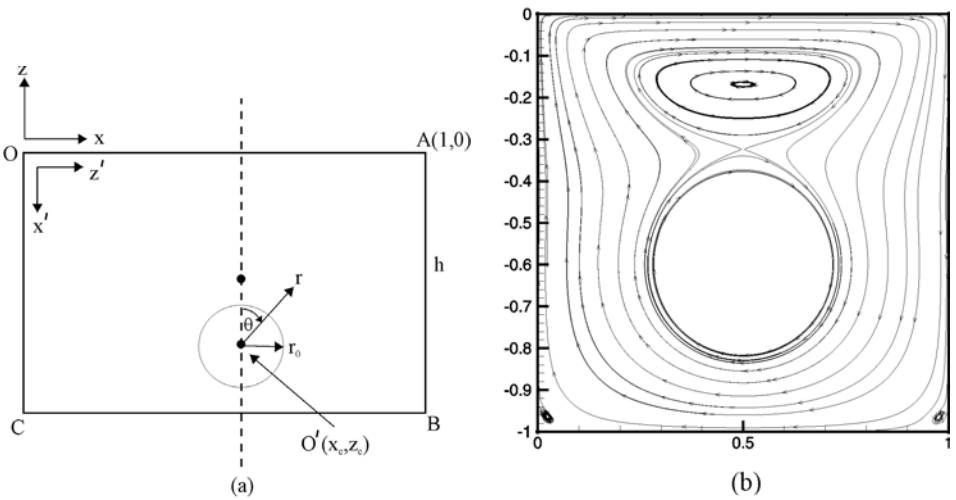

Figure 6. Stokes flow in a container with a rotating stirrer. **(a)** A schematic showing the coordinate systems used. **(b)** The streamline pattern when $h = 1, r_0 = 0.2, x_c = 0.5, z_c = -0.6, \delta = 0.1$ and $r_0\omega_0 = 0.5$. $N_1 = 100, N_2 = 50, M = 1000$.

the field is described by a stream function $\psi(x, z)$, such that $u_x = \psi_{,z}$ and $u_z = -\psi_{,x}$, which however now satisfies the biharmonic equation

$$\nabla^4\psi(x, z) = 0. \tag{3.15}$$

Now the embedding domain can be the rectangle OABC itself while the exterior eigenfunctions of (3.15) are naturally those that arise in cylindrical polar coordinates. In other words, we can write

$$\psi(x, z) = \psi^i(x, z) + \psi^e(r, \theta) + \psi^g(x, z), \tag{3.16}$$

where

$$\psi^i(x, z) = 2\Re\left[\sum_{n=1}^{N_1}\phi(x; \lambda_{2n-1})\{a_n e^{\lambda_{2n-1}z} + b_n e^{-\lambda_{2n-1}(h_1+z)}\} + \sum_{n=1}^{N_2}\phi(x'; \lambda_n)c_n\frac{\cosh\lambda_n(z' - \beta)}{\cosh\lambda_n\beta}\right], \tag{3.17a}$$

$$\psi^e(r, \theta) = d_0 r\ln r\cos\theta + e_0\ln r + (d_1 r^{-1} + e_1 r)\cos\theta + \sum_{n=2}^{N_2-1}\left\{d_n\left(\frac{r^*}{r}\right)^n + e_n\left(\frac{r^*}{r}\right)^{n-2}\right\}\cos n\theta, \tag{3.17b}$$

$$\psi^g(x, z) = f_1 z^2 + f_2 z^3 + f_3(x - 0.5)^2 + f_4(x - 0.5)^2 z, \tag{3.17c}$$

$$\sin\lambda_{2n-1} = -\lambda_{2n-1},\ \sin\lambda_{2n} = \lambda_{2n}, \quad n = 1, 2, \ldots. \tag{3.17d}$$

Note that (i) the exterior eigenfunctions again permit a slow growth and (ii) ψ^g is required to kill the inhomogeneous terms at the corners O, A, B and C. The complex scalars a_n, b_n and c_n and the reals d_n, e_n and f_1, f_2, f_3 and f_4 have to be determined by the least-squares procedure over M points on the boundary. The results of a typical calculation are shown in figure 6b. The lid speed is given in $1/2 \leq x \leq 1$ by $u_0(x) = 0.5\{1+\cos[\pi(x-(1-\delta))/\delta]\}$ for $(1-\delta) < x \leq 1$ and 1 for all other $x \geq 1/2$; i.e. uniform except for a smooth drop to the sidewall value. In this case the maximum error in a velocity component on the boundary was approximately 0.6×10^{-4}.

4. Conclusion

We have shown how the embedding method can be extended to cases where the domain is unbounded or multiply connected. The detailed examples given above show that the required extensions are conceptually simple and easy to implement. No attempt was made here to optimize the parameters that enter the procedure, for example the number of eigenfunctions used and the number of minimization points. As in the case of the embedding method itself, more experience will have to be gained to optimize these parameters for geometries that arise in actual applications.

References

[1] Filon L N G, The forces on a cylinder in a stream of viscous fluid, *Proc. R. Soc. London*, **A113** (1926) 7–27

[2] Miyagi T, Oseen flow past a circular cylinder, *J. Phys. Soc. Japan* **37** (1974) 1699–1707

[3] Shankar P N, On handling non-homogeneous corner data in confined steady Stokes flow, *Proc. R. Soc. London* **A460** (2004) 479–485

[4] Shankar P N, Eigenfunction expansions on arbitrary domains, *Proc. R. Soc. London* **A461** (2005) 2121–2133